

# Three-dimensional *ab initio* dipole moment surfaces and stretching vibrational band intensities of the $XH_3$ molecules\*

Liu An-Wen(刘安雯), Hu Shui-Ming(胡水明)<sup>†</sup>,  
Ding Yun(丁 昫), and Zhu Qing-Shi(朱清时)

Hefei National Laboratory for Physical Sciences at Microscale, Department of Chemical Physics,  
University of Science and Technology of China, Hefei 230026, China

(Received 10 March 2005; revised manuscript received 8 May 2005)

Stretching vibrational band intensities of  $XH_3$  ( $X=N, Sb$ ) molecules are investigated employing three-dimensional dipole moment surfaces combined with the local mode Hamiltonian model. The dipole moment surfaces of  $NH_3$  and  $SbH_3$  are calculated with the density functional theory and at the correlated MP2 level, respectively. The calculated band intensities are in good agreement with the available experimental data. The contribution to the band intensities from the different terms in the polynomial expansion of the dipole moments of four group V hydrides ( $NH_3$ ,  $PH_3$ ,  $AsH_3$  and  $SbH_3$ ) are discussed. It is concluded that the breakdown of the bond dipole approximation must be considered. The intensity “borrowing” effect due to the wave function mixing among the stretching vibrational states is found to be less significant for the molecules that reach the local mode limit.

**Keywords:** overtone, dipole moment, infrared band intensity, local mode

**PACC:** 3120A, 3310G, 3320E

## 1. Introduction

The quantum chemistry calculations have shed light on the area of molecular spectroscopy. The positions and intensities of ro-vibrational transitions can be predicted by correctly calculated potential energy surfaces (PES) and dipole moment surfaces (DMS). Up to now, the line positions can be calculated with a satisfactory accuracy by the variational calculations based on a sufficiently accurate PES. The recent progress on the calculated water vapour spectrum stands for a good example.<sup>[1,2]</sup> Based on an *ab initio* PES and followed by a careful adjustment according to the available observations of ro-vibrational transitions, the resulting PES can produce the energy levels below  $25000\text{ cm}^{-1}$  of variant isotopes of water with a sub  $1\text{ cm}^{-1}$  accuracy. However, it has also been found that the DMS model from quantum chemistry calculations often gives poor predictions for the intensities of high overtones.<sup>[3–10]</sup> About 3–10 times over- or under-estimation of the observed band intensities is

common. This is mainly due to the inaccurate high-order terms in the DMS, which would make significant contribution to the transitions in a highly excited energy region.<sup>[9–12]</sup> Meanwhile, the calculated intensities are found to be less sensitive to the potential energy surface.<sup>[7,12–15]</sup> In a previous paper, we studied the stretching overtones and combination bands of the  $XH_4$  ( $X=C, Si, Ge, Sn$ ) type group IV hydrides. By applying four-dimensional *ab initio* dipole moment surfaces and local mode potential energy surfaces, most of the observed band intensities were reproduced within a factor of 1.5.<sup>[16]</sup>

Here we concentrate on the group V hydrides ( $NH_3$ ,  $PH_3$ ,  $AsH_3$  and  $SbH_3$ ). The study has been carried out on  $PH_3$ ,<sup>[5]</sup> and  $AsH_3$ .<sup>[17]</sup> It is a fact that  $PH_3$ ,  $AsH_3$  and  $SbH_3$  are good local mode molecules whose stretching vibrational energy levels can be well described by the local mode theory, for instance, the anharmonically coupled anharmonic oscillator (ACAO) model. But it is not the case for  $NH_3$  because of complicated interactions like the strong

\*Project supported by the National Natural Science Foundation of China (Grant Nos 20103007 and 20473079).

<sup>†</sup>E-mail: smhu@ustc.edu.cn

Fermi resonance between the bending and stretching vibrations.<sup>[18]</sup> The potential energy surface parameters of NH<sub>3</sub> and SbH<sub>3</sub> have been calculated by local modes with Fermi resonance model,<sup>[18,19]</sup> by the effective normal mode model,<sup>[20]</sup> and also by the high level *ab initio* method.<sup>[21]</sup> Recently, six-dimensional PES and DMS were calculated at the CCSD(T) (coupled cluster theory with all single and double substitutions from the Hartree-Fock reference determinant<sup>[22]</sup> augmented by a perturbative treatment of connected triple excitations)<sup>[23,24]</sup> level, which could reproduce the experimental energy values of ammonia below 15000 cm<sup>-1</sup> with a deviation around 5 cm<sup>-1</sup>.<sup>[25]</sup> A global analytical representation of the electric dipole hyper-surface for ammonia is also introduced by Marquardt *et al.*<sup>[26]</sup> However, the local mode picture is also acceptable for the high overtones of NH<sub>3</sub>.<sup>[18]</sup> It is also a good approximation assuming the bending bands just “borrow” intensities from corresponding stretching bands through wave function mixing due to the Fermi Resonance. So it will be instructive to apply the crude local mode picture to NH<sub>3</sub> so as to compare it with other XH<sub>3</sub> species. In the present paper, the local mode Hamiltonian and stretching dipole moment models are given in Section 2, and the band intensities of SbH<sub>3</sub> and NH<sub>3</sub> are presented in Section 3. Section 4 includes discussion and concluding remarks.

## 2. Dipole moment and Hamiltonian models

The dipole moment vector  $\mathbf{M}$  is projected as

$$\mathbf{M}(r_1, r_2, r_3) = u_1(r_1, r_2, r_3)\mathbf{e}_1 + u_2(r_1, r_2, r_3)\mathbf{e}_2 + u_3(r_1, r_2, r_3)\mathbf{e}_3, \quad (1)$$

where  $\mathbf{e}_i$  ( $i = 1, 2, 3$ ) is the unit vector along the X-H<sub>*i*</sub> bond. Since XH<sub>3</sub> molecules belong to C<sub>3V</sub> point group, there are following relations for  $u_i$  ( $i = 1, 2, 3$ )

$$u_2(r_1, r_2, r_3) = u_1(r_2, r_1, r_3), \quad (2)$$

$$u_3(r_1, r_2, r_3) = u_1(r_3, r_2, r_1). \quad (3)$$

In this work, only the X-H bond stretching bands are considered, and  $u_1(r_1, r_2, r_3)$  is expanded with the polynomial functions in terms of the bond displacements ( $r_i, i = 1, 2, 3$ ),

$$u_1(r_1, r_2, r_3) = \sum_{i,j \geq k} C_{ijk}^B r_1^i (r_2^j r_3^k + r_2^k r_3^j) / (1 + \delta_{jk}), \quad (4)$$

where  $i, j$ , and  $k$  are non-negative integers,  $C_{ijk}^B$  is the expansion coefficient, and  $\delta_{jk}$  equals 1 if  $j = k$ , and

otherwise equals 0. Note that the expansion of the dipole moment function  $u_1$  can be divided into two parts:

$$u_1 = u_1^d + u_1^c, \quad (5)$$

$$u_1^d = C_{i00}^B r_1^i, \quad (6)$$

where  $u_1^d$  is the dipole moment (along the direction of the X-H<sub>1</sub> bond) introduced by a corresponding bond displacement, which is a polynomial function of  $r_1$ , we call it “diagonal” part. Another part  $u_1^c$  is referred to as “crossing” part. It comes into play when the displacements also happen to other bonds. In our recent paper on the XH<sub>4</sub> type molecules, we have pointed out that this part might be important and inappropriate to be neglected.<sup>[16]</sup>

The procedure of calculating the 3D X-H stretching DMS of XH<sub>3</sub> ( $X = \text{N, Sb}$ ) is similar to that used in the previous study on either PH<sub>3</sub><sup>[5]</sup> or AsH<sub>3</sub>.<sup>[17]</sup> It includes two steps: equilibrium geometry optimization, and single point calculation. The 3D DMS calculations are carried out with the B3PW91 method (Becke’s three parameter hybrid method with Perdew and Wang’s gradient-corrected correlation functional)<sup>[27,28]</sup> for NH<sub>3</sub>, and at the correlated MP2 level (second-order Møller–Plesset perturbation theory)<sup>[29]</sup> for SbH<sub>3</sub>, by using the GAUSSIAN 98 package.<sup>[30]</sup> The cc-pVQZ (correlation-consistent polarized valence quadruple zeta) basis set<sup>[31,32]</sup> is employed for the hydrogen and nitrogen atoms. The Hay and Wadt (HW)<sup>[33]</sup> effective core potentials are used with the corresponding double-zeta valence basis sets in a (3s3p)/[2s2p], augmented with one set of six Cartesian d polarization functions (the exponent<sup>[34]</sup> is 0.25) to the antimony atom. The optimized equilibrium geometry data compared with experimental values<sup>[35,36]</sup> are presented in Table 1. It is shown that our results are close to the experimental values. The dipole moments of NH<sub>3</sub> are calculated analytically in the B3PW91 implementation, while for SbH<sub>3</sub>, they are obtained by finite difference at the MP2 level with the equation which can be described by

$$M_i = \frac{E(p_i) - E(-p_i)}{2p_i}, \quad (7)$$

where  $i = x, y, z$ ,  $E(p_i)$  and  $E(-p_i)$  are, respectively, the correlated MP2 energies of SbH<sub>3</sub> molecule in the electric field with positive and negative strengths of  $p_i$  along the molecular fixed  $i$  axis,<sup>[8]</sup> and  $p_i$  is chosen to be 0.005 atomic units.

**Table 1.** Optimized and experimental equilibrium geometric structure of  $\text{NH}_3$  and  $\text{SbH}_3$ .

	$\text{NH}_3$		$\text{SbH}_3$	
	Cal.	Exp. <sup>a)</sup>	Cal.	Exp. <sup>b)</sup>
$R_{XH}/0.1\text{nm}$	1.0122	1.0166	1.6937	1.7000127
$\phi_{HXH}/(^{\circ})$	106.66	106.68	91.5652	91.55662

<sup>a)</sup>From Ref.[35]. <sup>b)</sup>From Ref[36].

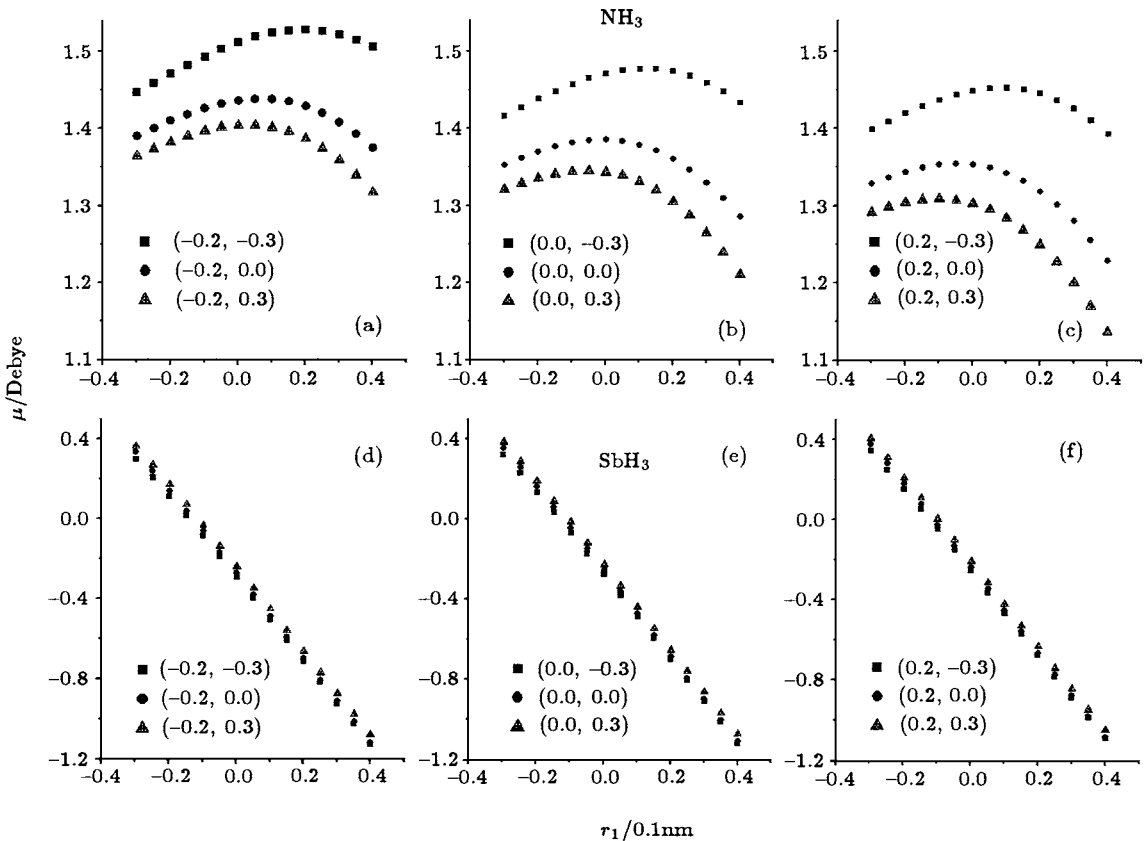
The method to fit the 3D DMS is referred to Ref.[5]. It is shown that it is unnecessary to include many high order terms in the fit of the three-dimensional DMS.<sup>[9]</sup> All terms with higher than fourth order are neglected here, and the  $C_{021}^B$  of  $\text{NH}_3$  and  $\text{SbH}_3$  are also constrained to zero for the same reason. The expanded coefficients of  $\text{NH}_3$  and  $\text{SbH}_3$  are given in Table 2. Figure 1 provides parts of the *ab initio* calculated dipole moments along the  $X\text{-H}_1$  ( $X=\text{N}, \text{Sb}$ ) bond to show the difference between  $\text{NH}_3$  and  $\text{SbH}_3$ . The dipole moments along the  $X\text{-H}_1$  bond at different fixed values of  $r_2$  and  $r_3$  show nonlinear dependence on the  $r_1$  value for  $\text{NH}_3$ , while quite linear for  $\text{PH}_3$ ,<sup>[5]</sup>  $\text{AsH}_3$ ,<sup>[37]</sup> and  $\text{SbH}_3$ . Particularly, it is clearly shown that when  $r_1$  is fixed the dipole moment along the  $X\text{-H}_1$  bond of  $\text{NH}_3$  varies markedly at different values of  $r_2$  and  $r_3$ . Note that the upper and lower panels in this figure have different vertical scales, we shall point out

that actually, it is almost the same situation as  $\text{SbH}_3$ . It is interesting to note that a similar phenomenon is also found in  $\text{XH}_4$  type hydrides.<sup>[16]</sup>

**Table 2.** Three-dimensional stretching vibrational DMS coefficients of  $\text{NH}_3$  and  $\text{SbH}_3$ .\*

	$\text{NH}_3$	$\text{SbH}_3$
$C_{000}$	1.373413(65)	-0.259647(30)
$C_{100}$	-0.03718(39)	-2.13842(17)
$C_{010}$	-0.17436(22)	0.09295(16)
$C_{200}$	-0.51644(95)	-0.16489(43)
$C_{020}$	0.25334(75)	0.07070(42)
$C_{110}$	-0.27934(79)	-0.04449(36)
$C_{011}$	-0.14499(65)	-0.01970(30)
$C_{300}$	-0.2832(39)	0.5039(17)
$C_{030}$	0 <sup>a)</sup>	-0.0839(17)
$C_{210}$	-0.3358(33)	0.0816(15)
$C_{021}$	0 <sup>a)</sup>	0 <sup>a)</sup>
$C_{120}$	0.2985(33)	0.2472(15)
$C_{111}$	-0.3029(28)	-0.0359(13)
rms <sup>b)</sup> /10 <sup>-3</sup>	1.91	0.84

\* Units are defined as follows: the dipole moment is in Debye ( $= 3.33564 \times 10^{-30}$  C m), the bond length displacement is in 0.1nm. The value in each parenthesis is one standard error in the last significant digit. <sup>a)</sup> Constrained values. <sup>b)</sup> Root mean squares of the fitting residual.

**Fig.1.** The dipole moments along the  $X\text{-H}_1$  bond in  $\text{NH}_3$  and  $\text{SbH}_3$  according to the bond length displacement  $r_1$  at different values of  $r_2$  and  $r_3$  respectively. Values in parentheses are for  $r_2$  and  $r_3$ . The upper and lower panels are for  $\text{NH}_3$  and  $\text{SbH}_3$ , respectively.

The ACAO I model is used to calculate the vibrational wavefunctions:

$$H = \sum_{i=1}^3 \left( \frac{1}{2} G_{rr} p_i^2 + D_e y_i^2 \right) + \sum_{i<j} (G_{rr'} p_i p_j + F_{rr'} r_i r_j). \quad (8)$$

Here  $m_H$  and  $m_X$  are the mass of the H and X atoms, respectively,  $\phi$  is the experimental equilibrium value for the H-X-H angle,  $p_i$  is the momentum conjugate to  $r_i$ ,  $D_e$  and  $\alpha$  are the Morse potential parameters, and  $F_{rr'}$  is the inter-bond potential coupling parameter. For  $\text{NH}_3$ , the parameters  $D_e$  and  $\alpha$  are optimized by the least-squares fitting to thirteen observed vi-

brational band centers, while  $F_{rr'}$  is constrained to the calculated value by Esa Kauppi *et al.*<sup>[18]</sup> The results are  $D_e = 41535(326) \text{ cm}^{-1}$ ,  $\alpha = 2.0560(106) (0.1 \text{ nm})^{-1}$ , and  $F_{rr'} = 455.08 \text{ cm}^{-1} (0.1 \text{ nm})^{-2}$ , where the value in each parenthesis is one standard error in units of the last quoted digit. The root mean square of the fitting residual is  $16.8 \text{ cm}^{-1}$ . For  $\text{SbH}_3$ , the effective parameters are  $D_e = 28566(52) \text{ cm}^{-1}$ ,  $\alpha = 1.4135(17) (0.1 \text{ nm})^{-1}$ ,  $F_{rr'} = -191(56) \text{ cm}^{-1} (0.1 \text{ nm})^{-2}$ , and the root-mean-square of the fitting residual is  $1.94 \text{ cm}^{-1}$ . The deviations from the observed values of the band centers of  $\text{NH}_3$  and  $\text{SbH}_3$  are presented in Table 3.

**Table 3.** Observed and calculated stretching vibrational band centers (in  $\text{cm}^{-1}$ ) and calculated band intensities (in  $10^{-22} \text{ cm}^2/\text{molec}$ ) of  $\text{NH}_3$  and  $\text{SbH}_3$ .

band	$\text{NH}_3$				$\text{SbH}_3$			
	$\nu_{\text{obs}}$ <sup>a)</sup>	$\nu_{\text{calc}}$	$\delta_{\text{o-c}}$	$I_{\text{cal}}$	$\nu_{\text{obs}}$ <sup>b)</sup>	$\nu_{\text{calc}}$	$\delta_{\text{o-c}}$	$I_{\text{cal}}$
(100; $A_1$ )	3336.2	3337.5	-1.3	$0.514 \times 10^4$	1890.502	1890.789	-0.29	$0.246 \times 10^6$
(100; $E$ )	3443.4	3426.9	16.5	$0.166 \times 10^4$	1894.497	1896.425	-1.93	$0.701 \times 10^6$
(200; $A_1$ )	6606.0	6593.5	12.5	$0.370 \times 10^4$	3719.933	3721.197	-1.26	$0.443 \times 10^4$
(200; $E$ )	6609.2	6635.2	-26.0	$0.310 \times 10^4$	3719.860	3721.605	-1.74	$0.993 \times 10^4$
(110; $A_1$ )	6796.0	6810.5	-14.5	$0.244 \times 10^3$		3785.505		$0.584 \times 10^2$
(110; $E$ )	6850.4	6833.1	17.3	$0.385 \times 10^2$		3790.799		$0.147 \times 10^2$
(300; $A_1$ )		9713.8		$0.520 \times 10^4$	5480.285	5481.248	-0.96	$0.926 \times 10^2$
(300; $E$ )	9689.8	9722.5	-32.7	$0.184 \times 10^3$	5480.235	5481.263	-1.03	$0.991 \times 10^2$
(210; $A_1$ )		9939.6		$0.690 \times 10^4$	5607	5609.560	-2.56	$0.100 \times 10^2$
(210; $lE$ )		10002.3		$0.500 \times 10^4$		5612.481		$0.268 \times 10^4$
(210; $hE$ )		10093.1		$0.330 \times 10^2$		5619.014		$0.335 \times 10^4$
(400; $A_1$ )		12665.2		$0.900 \times 10^0$	7173.799	7173.600	0.20	$0.250 \times 10^4$
(400; $E$ )	12675.5	12666.2	9.3	$0.145 \times 10^2$	7173.783	7173.601	0.18	$0.153 \times 10^0$
(310; $A_1$ )		13043.2		$0.300 \times 10^0$		7372.465		$0.643 \times 10^0$
(310; $lE$ )		13085.0		$0.110 \times 10^4$		7373.048		$0.160 \times 10^{-2}$
(310; $hE$ )		13139.1		$0.200 \times 10^4$		7376.484		$0.453 \times 10^0$
(500; $A_1$ )	15449.1	15459.0	-9.9	$0.138 \times 10^0$		8798.525		$0.719 \times 10^{-1}$
(500; $E$ )	15449.9	15459.1	-9.2	$0.145 \times 10^4$		8798.525		$0.125 \times 10^0$
(410; $A_1$ )		16018.1		$0.240 \times 10^{-1}$		9064.979		$0.428 \times 10^{-1}$
(410; $lE$ )		16030.8		$0.200 \times 10^0$		9065.010		$0.153 \times 10^{-2}$
(410; $hE$ )		16085.6		$0.770 \times 10^{-1}$		9068.758		$0.323 \times 10^{-1}$
(600; $A_1$ )	18109.3	18100.3	9.0	$0.230 \times 10^{-1}$	10358	10356.034	2	$0.148 \times 10^{-2}$
(600; $E$ )	18108.5	18100.3	8.2	$0.179 \times 10^0$	10358	10356.035	2	$0.533 \times 10^{-1}$
(510; $A_1$ )		18822.7		$0.200 \times 10^{-2}$		10689.623		$0.360 \times 10^{-2}$
(510; $lE$ )		18824.7		$0.210 \times 10^{-1}$		10689.624		$0.200 \times 10^{-3}$
(510; $hE$ )		18885.0		$0.600 \times 10^{-2}$		10693.389		$0.290 \times 10^{-2}$

<sup>a)</sup> From Ref.[18]. <sup>b)</sup> From Ref.[19].

### 3. Calculated stretching band intensities

The absolute vibrational band intensity can be calculated by

$$I = \frac{8\pi^3\nu_0}{3hcQ_v(T)} \left[ 1 - \exp\left(-\frac{h\nu_0}{kT}\right) \right] \nu_0 |\langle N | \mathbf{M} | 0 \rangle|^2 \doteq K\nu_0 |\langle N | \mathbf{M} | 0 \rangle|^2, \quad (9)$$

where  $|0\rangle$  and  $|N\rangle$  denote the vibrational ground and excited states respectively,  $\nu_0$  is the band center in  $\text{cm}^{-1}$ ,  $Q_v(T)$  is the vibrational partition function at temperature  $T$ ,  $c$  is the speed of light,  $h$  and  $k$  are Planck and Boltzmann constants, respectively. The approximation in the second line of Eq.(9) is fulfilled since  $Q_v(T) \doteq 1$  and  $\exp\left(-\frac{h\nu_0}{kT}\right) \ll 1$  under the present conditions. The constant  $K$  equals  $4.1623755 \times 10^{-19} \text{ cm}^2 \text{ Debye}^{-2}$  (1 Debye =  $3.33564 \times 10^{-30} \text{ C m}$ ).

#### 3.1. SbH<sub>3</sub>

The calculated absolute band intensities of SbH<sub>3</sub> are listed in the column 7 in Table 3. Due to the lack of observed data, we only compare the relative band intensities which are calculated by

$$I_{\text{rel}}(i) = \frac{I_{\text{abs}}(i)}{I_{\text{abs}}(100)}, \quad (10)$$

where  $I_{\text{rel}}(i)$  and  $I_{\text{abs}}(i)$  are the relative and absolute intensities of the band  $i$ , respectively.  $I_{\text{abs}}(100)$  is the overall intensity of bands (100,  $A_1$ ) and (100,  $E$ ). The calculated and observed relative band intensities are given in columns 2 and 3 of Table 4. For the first and second overtone bands, our calculated values are in good agreement with the experimental values given by Ref.[38], and the accuracy is similar to the one calculated from an empirical bond dipole model in the same reference (values also given in the column 4 of Table 4). For the third overtone, our result is only one fifth of the experimental value and the empirical bond dipole model gives one half. But for the combination band (210,  $A_1$ ), we reproduce the experimental band intensity very well, while the value obtained by the empirical bond dipole model is more than one hundred times smaller. Actually, the relative intensities of combination bands calculated by the empirical bond dipole model<sup>[38,39]</sup> have large differences from the observed values for both AsH<sub>3</sub> and SbH<sub>3</sub>. This may result from the inappropriate neglect of the con-

tribution from inter-bond coupling terms in their dipole moment model.

**Table 4.** Observed and calculated relative band intensities of SbH<sub>3</sub>.

band	$I_{\text{obs}}^{\text{a)}$	$I_{\text{cal}}^{\text{a)}$	$I_{\text{cal}}^{\text{b)}$
(100, $A_1/E$ )	1.0	1.0	1.0
(200, $A_1/E$ )	0.022	0.015	0.021
(300, $A_1/E$ )	$0.32 \times 10^{-3}$	$0.47 \times 10^{-3}$	$0.20 \times 10^{-3}$
(210, $A_1$ )	$0.11 \times 10^{-4}$	$0.82 \times 10^{-7}$	$0.11 \times 10^{-4}$
(400, $A_1/E$ )	$0.14 \times 10^{-4}$	$0.78 \times 10^{-5}$	$0.28 \times 10^{-5}$

a) From Ref.[38]. b) This work.

#### 3.2. NH<sub>3</sub>

The observed and calculated vibrational energy levels, along with the band intensities calculated from the DFT DMS are listed in columns 2, 3 and 4 in Table 3. It is not surprising that there are large discrepancies between the observed and calculated energy levels since the strong Fermi resonance and inverse splitting are not included in our simple ACAO model. For the band intensities of NH<sub>3</sub>, to the best of our knowledge, the available experimental data on band intensities is surprisingly limited. The intensities of the (100,  $A_1$ ) and (100,  $E$ ) bands were determined by Kleiner *et al.*<sup>[40]</sup> they are 9498 and 4747 (in units of  $10^{-22} \text{ cm/Molecule}$ ), respectively. Coy and Lehmann<sup>[41]</sup> gave the line intensities for 39 and 15 prominent lines in the five and six quanta bands, respectively. The summed values of the intensities of these prominent lines can be considered as an estimation of the lower limit of the band intensities. They are 0.455 for the (500,  $A_1/E$ ) band and 0.041 (in unit of  $10^{-22} \text{ cm/molecule}$ ) for the (600,  $A_1/E$ ) band. The calculated intensities of (100,  $A_1$ ) and (100,  $E$ ) are 2–3 times smaller than these available experimental values, which may result from the deviation of the wave functions since the ACAO model should not describe the low excited vibrational states of NH<sub>3</sub>. Our calculated intensities of (500,  $A_1/E$ ) and (600,  $A_1/E$ ) bands are about triple larger than the experimental values. The discrepancy seems large here, but on the one hand, the discrepancy should be much smaller since the “experimental” intensities we used here are most likely lower limits of the true values, on the other hand, as a rough estimation on the difficult issue of the band intensities, such discrepancy is already acceptable. We expect more experimental data, especially for the high excited overtones and combination bands to be available to test the result listed in Table 3.

## 4. Discussion and conclusions

In the earlier work,<sup>[16]</sup> we discussed the contributions to the overtone transition moments from diagonal and crossing terms in the polynomial expansion of the dipole moments according to the bond displacements. Actually, if we take a “bond dipole” approximation, which means that the assumption is made that the “crossing” terms are all negligible and only the “diagonal” terms remain in the dipole moment expansion, then the vibration induced dipole moment must be aligned with the vibrating bond. This approximation is simple but as we have examined in the study on the group IV hydrides  $XH_4$  ( $X=C, Si, Ge, Sn$ ), large deviation will be found if the crossing terms are neglected, particularly when the combination bands are considered. For those contributions from such crossing terms, as the breakdown of the “bond dipole” approximation, we call it “crossing” effect. Another effect is the so-called “borrowing” effect, which comes from the wave function mixing. Due to the miscellaneous vibrational interaction resonance or the complexity of the potential energy surface, each vibrational state will not be a “pure” local-mode vibration state but a combination of all interacting states. As a consequence, the transition moments will be re-distributed among all the interacting vibrational bands. For example, a “dark” combination band could “borrow” some strengths from other “bright” bands, for example, the corresponding overtone within the same vibrational polyad. We believe that, for those molecules which could be well described by the local-mode model, like  $SiH_4$ ,  $GeH_4$ , and  $SnH_4$  in the group IV hydrides and  $PH_3$ ,  $AsH_3$ , and  $SbH_3$  in the group V hydrides discussed in present paper, the “borrowing” effect will be less important when the energy grows up or the local-mode limit is reached. Since  $NH_3$  and  $CH_4$  are not such local-mode molecules, for those molecules the local mode model is poor to describe the vibrational states, there by the “borrowing” effect will remain significant.

In order to understand the origin of the stretching vibrational band intensities of the polyatomic hydrides, we focus on the investigation of the “crossing” and “borrowing” effects, and calculate the contributions to the band intensities from different terms for the  $XH_3$  ( $X=N, P, As, Sb$ ) molecules. Three cases

which correspond to three different limits are considered: 1)  $I_1$  is the intensity calculated when the “borrowing” effect is neglected, and the wave function of the upper energy state is assumed to be a “pure” local-mode state; 2)  $I_2$  is the intensity calculated when the “crossing” effect is neglected, the dipole function is simplified into a bond dipole function, and all crossing terms in the DMS expansion are neglected, while the “borrowing” effect is included; 3)  $I_3$  is the intensity calculated on the assumption that only the crossing terms in the DMS expansion are important and all other diagonal terms are neglected. For each case, the intensities of the overtones—from the ground state to the  $(n\ 0\ 0)$  states, and of the usually strongest combination bands in each polyad—from the ground state to the  $(n-1\ 1\ 0)$  states, are calculated. The resulting values are then normalized to the true values when both the “borrowing” and “crossing” effects are included. The results of  $(n\ 0\ 0)$  overtones and  $(n-1\ 1\ 0)$  combinations are shown in the upper and lower panels of Fig.2, respectively. The following points can be concluded from the figure: (1) The “borrowing” effect can be neglected for the  $(n\ 0\ 0)$  overtones of all these molecules and also for the combination bands of local mode molecules ( $PH_3$ ,  $AsH_3$  and  $SbH_3$ ) when close to the local-mode limit ( $n > 2$ ). The “borrowing” effect seems to be only accountable in the combination bands of  $NH_3$ . This point can be easily concluded from plots *a* and *b*. (2) For the overtones, both the diagonal and “crossing” terms in the DMS expansion are important for most molecules (plots *c* and *e*). The “crossing” effect is the leading contribution to the high excited combination bands which is clearly shown in plots *e* and *f*.

So we may conclude that the “crossing” effect is the leading contribution to the combination bands and also an important part to the overtones for most  $XH_n$  type hydrides. When we limit our discussion to the band intensity distribution among different stretching bands within a polyad, the “borrowing” effect seems negligible for the molecules in the local-mode limit, for example, high vibrational excited states of  $PH_3$ ,  $AsH_3$ , and  $SbH_3$  in the present discussion. We think it can be also considered as an alternative character for the molecule reaching the local-mode limit other than the pattern of energy levels.

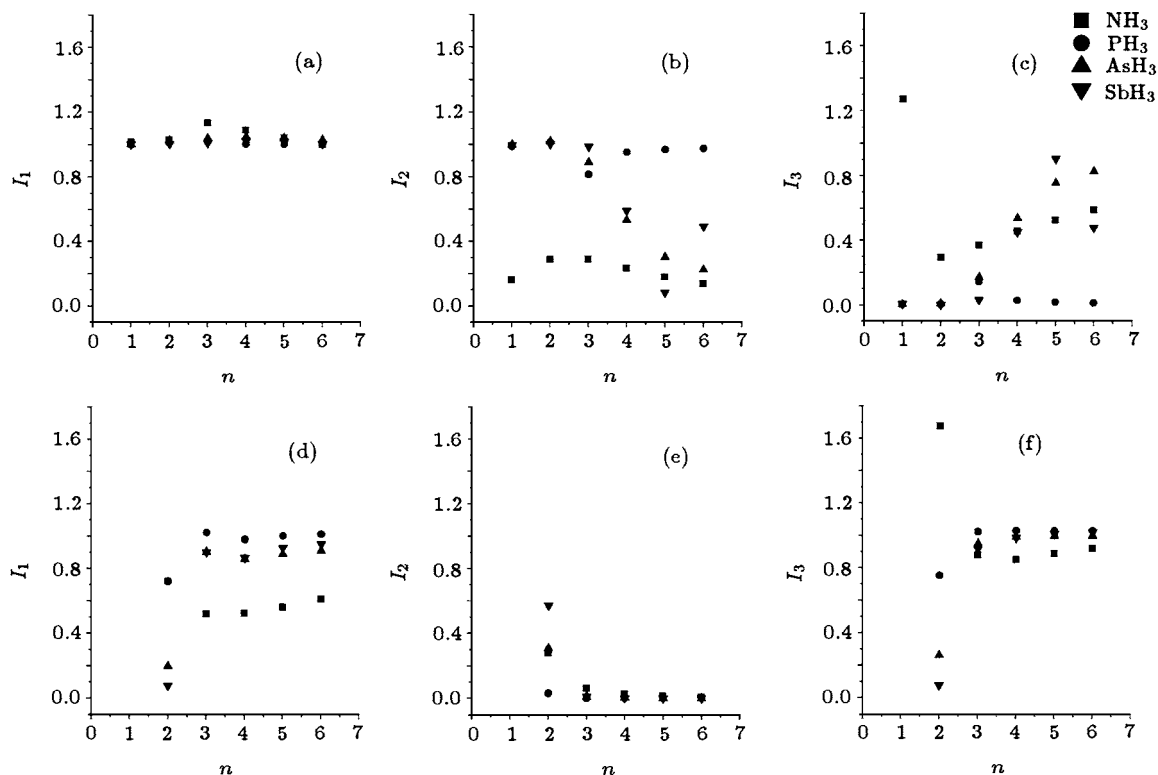


**Fig.2.** The relative contributions to the band intensities, calculated in three cases (see in text). The upper panels are for the  $(n\ 0\ 0)$  overtones, and the lower panels are for the  $(n-1\ 1\ 0)$  combination bands.

## References

- [1] Partridge H and Schwenke D W 1997 *J. Chem. Phys.* **106** 4618
- [2] Shirin S V, Polyansky O L, Zobov N F, Barletta P and Tennyson J 2003 *J. Chem. Phys.* **118** 2124
- [3] Lin H, Bürger H, He S G, Yuan L F, Breidung J and Thiel W 2001 *J. Phys. Chem. A* **105** 6065
- [4] He S G, Lin H, Bürger H, Thiel W, Ding Y and Zhu Q S 2002 *J. Chem. Phys.* **116** 105
- [5] He S G, Zheng J J, Hu S M, Lin H, Ding Y, Wang X H and Zhu Q S 2001 *J. Chem. Phys.* **114** 7018
- [6] He S G, Lin H, Thiel W and Zhu Q S 2001 *Chem. Phys. Lett.* **349** 131
- [7] Lin H, Yuan L F, He S G and Wang X G 2001 *J. Chem. Phys.* **114** 8905
- [8] Lin H, He S G, Wang X G, Yuan L F, Bürger H, D'Eu J F, Reuter N and Thiel W 2001 *Phys. Chem. Chem. Phys.* **3** 3506
- [9] Lin H, Bürger H, Mkadmi E B, He S G, Yuan L F, Breidung J, Thiel W, Huet T R and Demaison J 2001 *J. Chem. Phys.* **115** 1378
- [10] He S G, Yuan L F, Lin H, Zhu Q S and Wang X G 2001 *J. Phys. Chem. A* **105** 8428
- [11] Lin H, Yuan L F, He S G, Wang X G and Zhu Q S 2000 *J. Chem. Phys.* **112** 7484
- [12] Kjaergaard H G and Henry B R 1992 *J. Chem. Phys.* **96** 4841
- [13] Lewerenz M and Quack M 1986 *Chem. Phys. Lett.* **123** 197
- [14] Ha T K, Lewerenz M, Marquardt R R and Quack M 1990 *J. Chem. Phys.* **93** 7097
- [15] Fair J R, Votava O and Nesbitt D J 1998 *J. Chem. Phys.* **108** 72
- [16] He S G, Liu A W, Lin H, Hu S M, Zheng J J, Hao L Y and Zhu Q S 2002 *J. Chem. Phys.* **117** 10073
- [17] Zheng J J, He S G, Ding Y, Hao L Y, Wang X H, Hu S M and Zhu Q S 2002 *Chem. Phys. Lett.* **352** 435
- [18] Kauppi E and Halonen L 1995 *J. Chem. Phys.* **103** 6861
- [19] Lummila J, Lukka T, Halonen L, Bürger H and Polanz O 1996 *J. Chem. Phys.* **104** 488
- [20] Lehman K K and Coy S L 1988 *J. Chem. Soc. Faraday Trans.* **84** 1389
- [21] Breidung J and Thiel W 1995 *J. Mol. Spectrosc.* **169** 166
- [22] Purvis G D and Bartlett R J 1982 *J. Chem. Phys.* **76** 1910
- [23] Urban M, Noga J, Cole S J and Bartlett R J 1985 *J. Chem. Phys.* **83** 4041
- [24] Raghavachari K, Trucks G W, Pople J A and Head-Gordon M 1989 *Chem. Phys. Lett.* **157** 479
- [25] Lin H, Thiel W, Yurchenko S N, Carvagal M and Jensen P 2002 *J. Chem. Phys.* **117** 1
- [26] Marquardt R, Quack M, Thanopoulos I and Luckhaus D 2003 *J. Chem. Phys.* **119** 10724
- [27] Becke A D 1993 *J. Chem. Phys.* **98** 5648
- [28] Perdew J P and Wang Y 1995 *Phys. Rev. B* **45** 13244
- [29] Møller C and Plesset M S 1934 *Phys. Rev.* **46** 618

- [30] Frisch M J 1998 *GAUSSIAN 98, Revision A.9* (Pittsburgh, PA: Gaussian Inc.)
- [31] Dunning T H 1989 *J. Chem. Phys.* **90** 1007
- [32] Woon D E and Dunning T H 1993 *J. Chem. Phys.* **98** 1358
- [33] Hay P J and Wadt W R 1985 *J. Chem. Phys.* **82** 270
- [34] Breidung J and Thiel W 1992 *J. Comput. Chem.* **13** 165
- [35] Callomon J H, Hirota E, Kuchitsu K, Lafferty W J, Maki A G and Pote C S 1976 *Landolt-Bornstein, Structure Data of Free Polyatomic Molecules*, edited by Hellwege K H and Hellwege M A (Berlin: Springer) Vol.II.
- [36] Fusina L, Di Lonardo G and De Natale P 1998 *J. Chem. Phys.* **109** 997
- [37] Zheng J J 2002 *Study on the High Resolution Infrared Molecular Spectroscopy* (Ph.D. Thesis, University of Science and Technology of China)
- [38] Halonen M, Halonen L, Bürger H and Moritz P 1992 *J. Phys. Chem.* **96** 4225
- [39] Child M S and Halonen L 1984 *Adv. Chem. Phys.* **57** 1
- [40] Kleiner I, Brown L R, Tarrago G, Kou Q L, Picque N, Guelachvili G, Dana V and Mandin J Y 1999 *J. Mol. Spectrosc.* **193** 46
- [41] Coy S L and Lehmann K K 1986 *J. Chem. Phys.* **84** 5239